Passive longitudinal-phase-space tailoring of non-ultrarelativistic beams with dielectric-lined waveguides

F. Lemery* and P. Piot*,†

*Northern Illinois Center for Accelerator & Detector Development and Department of Physics, Northern Illinois University, DeKalb IL 60115, USA
†Accelerator Physics Center, Fermi National Accelerator Laboratory, Batavia, IL 60510, USA

Abstract. To date conventional use of dielectric-lined waveguides (DLWs) has mainly concerned high-gradient acceleration. In this paper we investigate an alternative use of such waveguides to impressed wakefield-induced energy correlations on non-ultra-relativistic beams. These correlations are shown to produce density modulations as the beam drifts in a free space. We explore several schemes with a single or multiple DLW structures which can lead to passive compressions and to the formation of sub-picosecond bunch trains. We finally suggest the possible use of multiple structures to bunch the beam at higher frequencies using a scheme similar to a two-stage echo enabled harmonic generation.

Keywords: beam-driven acceleration, wakefield, bunch compression, beam echo
PACS: 29.27.-a, 41.85.-p, 41.75.F

INTRODUCTION

Dielectric lined waveguides (DLW) have been shown of generating large (> 1 GV/m) accelerating gradients from high charge (> 1 nC) electron bunches [1]. In such a scheme, a "drive" bunch passes through a DLW (e.g. tube, or slab structure), and excites an electromagnetic wake which depends on the longitudinal bunch shape. To maximize acceleration gradients, the bunch length σ_z should be less than half of the fundamental wavelength λ_0 of the structure ($\sigma_z < \lambda_0/2$) such that the bunch is entirely decelerated. However, in the regime where $\sigma_z >> \lambda_0$, a flat-top bunch for example, will experience a quasi-sinusoidal energy modulation which can be converted into a density modulation with a proper dispersive section [4].

In this paper we explore the use of DLWs with low energy ($\mathscr{E} < 10$ MeV) electron beams typically produced in radiofrequency (RF) photoinjectors. In such a setup, the electron bunches produced can be manipulated with the laser and RF systems, leading to flexibility in charge, beam energy, emittances, and bunch lengths. Additionally, due to the relatively low energies of the beam, energy modulations can be converted to density modulations as the drift space of length L has a longitudinal dispersion $R_{56} = L/\gamma^2$. We extend the study presented in Ref. [2], and discuss the use of DLW's as passive structures capable of enabling an array of dynamic beam manipulation techniques. We exemplify the use of a DLW as a passive compressor, or bunch shaper. Additionally we explore the use of multiple DLW structures to enable a mechanism similar to echo enabled harmonic generation [6].

To support our studies, we consider the case of a 1 nC bunch produced out of a photoinjector electron source similar to the LCLS RF-gun [7], although in principle more conventional guns (e.g. L-Band) are capable of generating similar results. The large advantages of S-Band over L-Band are the larger accelerating fields on the cathode which generally lead to smaller emittances which reduces the difficulty of fitting into DLWs. We use the program ASTRA to carry particle-tracking simulations taking into account the effects of space charge. For the simulations presented in this paper, we use a cylindrical-symmetric space charge algorithm [9] and represent the bunch with 50,000 macro particles. The use of the 2+1/2 space-charge algorithm is legitimate as the setup under consideration includes elements (solenoidal lenses, RF-gun, and DLW structures) that are all cylindrical symmetric.

The wakefield interactions with the beam is calculated via a Green's function approach [8] where the bunch current is convolved with the Green's function of the structure; the resulting decelerating field is applied to the bunch and scaled by the length of the structure. In the report we exclusively consider cylindrically-symmetric DLW consisting of a hallow material of inner and outer radii a and b respectively. The outer surface of the waveguide is contacted to a

perfect conductor. In our simulations we do not take into account any dipole modes which would introduce transverse kicks; these modes are negligible as long as the beam is centered through the DLWs.

BUNCH COMPRESSION

Magnetic bunch compression is a wide-spread method to enhance the peak current of electron bunches. The technique employs a dispersive section producing a longitudinal dispersion so that an incoming bunch with a properly tuned energy chirp has an upright longitudinal phase space downstream of the dispersive section. This technique is commonly employed in electron linac and routinely achieves multi-kA peak current, however it suffers from collective effect arising from coherent synchrotron radiation (CSR). An alternative approach is to compress the beam at low energies, where an energy-modulated beam can ballistically compress in a drift space. At low energy however, space charge affects the beam quality, as bunching leads to large fields which degrade bunching and results in an increase of the beam's energy spread. Ballistic bunching is often employed in electron injectors [10, 12, 13] and was recently applied in ultra-fast electron-diffraction experiments to produce sub 30-fs electron bunches [14]. Typically the required energy correlation is imparted using an accelerating RF cavity operated at zero-crossing.

In the work presented in Ref. [2], we essentially focused on the production of high-peak-current bunches to the sacrifice of the population being compressed (e.g. in some case we had only $\sim 7\%$ of the bunch population compressed with a 12-kA spike). It is however sometime more valuable to compress a larger portion of bunch.

As an example, we first consider a Gaussian bunch "tail-bunching," where $4\sigma_z \sim \lambda_0/2$. In this regime, the rear half of the bunch acquires a quasi-linear negative chirp which leads to a compression after a drift of proper length. In Fig. 1(left) we present results for a DLW with dimensions $(a,b) = (1\text{ mm}, 1.05\text{ mm})$, relative dielectric permittivity $\varepsilon_r = 5.7$, (corresponding to the fundamental-mode wavelength $\lambda_0 = 0.974$ mm) and length $L = 5$ cm. Such a configuration leads to $\sim 50\%$ of the bunch population compressing into 100-μm full-width spike.

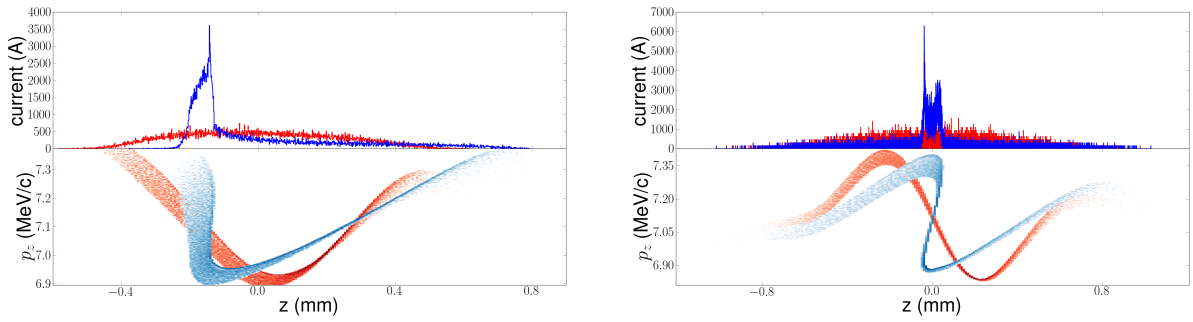

FIGURE 1. Example of bunch-tail (left) and central (right) bunching. For each cases, the current (top) and longitudinal phase space (bottom) are shown immediately downstream of the DLW (red trace), and 1.2 m (left) or 1.13 m (right) downstream of the DLW (blue trace).

Another choice is to modulate the bunch in the regime where $4\sigma_z = \lambda_0$, so that the largest concentration of charge (e.g. centrally for a symmetric bunch) is compressed. Again we explore a Gaussian bunch, now with full bunch length $4\sigma_z \sim 1.7$ mm and a DLW with dimensions $(a,b) = (0.8\text{ mm}, 0.85\text{ mm})$ which leads to $\lambda_0 = 0.887$ mm. The length of the structure is doubled to $L = 10$ cm for these simulations. In this simulation, a maximum of 55.8% is found in the 100-μm full-width spike 1.13 m downstream of the DLW; see Fig. 1 (right). In principle this technique could also be scaled to longer wavelengths and bunch lengths while increasing the bunch charge.

It should be noted that this technique relies on the non ultra-relativistic nature of the bunch and that the compressed bunch shapes presented in Fig. 1 are achieved at a given axial location and are still evolving. In order to freeze the bunch shape, e.g. for use at higher energy, the beam need to be accelerated and the DLW parameter would need to be optimized to include the effect of downstream acceleration. Finally, a key feature to the bunch compression is the local (or intrinsic) fractional momentum spread. As seen in Fig. 1 (red traces in the longitudinal phase space), the slice

energy spread depends on the axial slice considered. Therefore being able to control the slice energy spread at a given axial location (i.e. that matches the zero-crossing in the correlated energy spread imparted by the DLW) could lead to higher peak current containing larger amount of charge.

BUNCH-CURRENT SHAPING

To date, few methods have been demonstrated and proposed to produce longitudinally-shaped drive bunches for enhanced transformer ratio applications. Possible methods include the use of a shaped mask in a dispervise section [15, 16], the mapping of a transversely-shaped beam into the temporal axis using a transverse-to-longitudinal phase-space exchanger [17] or the use of nonlinear longitudinal manipulation [18, 19]. Here we point out that the passive technique described in the this paper can be used to form beams with tailored current profiles. In such a scheme, the combined effects of longitudinal-phase-space curvatures induced by the DLW with the relative motion of the electrons within the bunch results in nonlinear phase space distortions that can lead to the formation of ramped current profile as proposed and observed in linacs combined with bunch compressors [19].

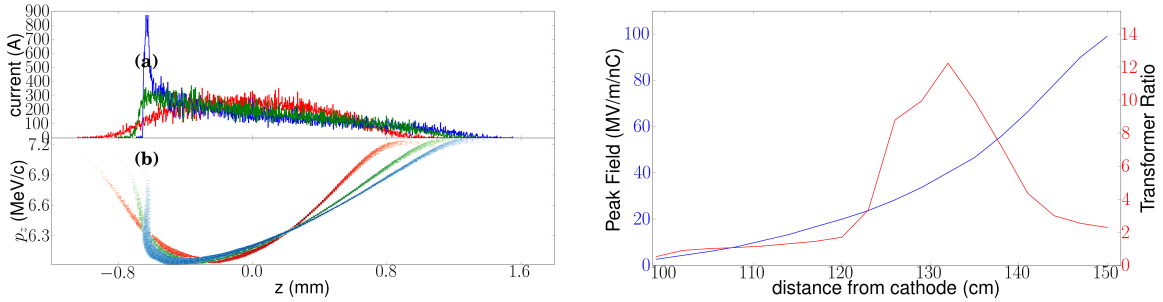

FIGURE 2. Snapshots of the longitudinal phase spaces (lower left) and associated bunch currents (upper left) simulated immediately after the DLW (red), 35 cm (green) and 50 cm (blue) downstream of the DLW structure. Evolution of the peak accelerating field and transformer ratio (right) calculated along the axial drift (see text for details).

We use a DLW and consider the maximum accelerating gradient (E_+) behind the bunch and the transformer ratio (defined as $\mathscr{R} = E_+/E_-$ where E_- is the peak decelerating field within the bunch) in the simulations. The choice of DLW parameters to induce the required energy modulation needed to eventually produce a linearly-ramped bunch depends foremost on the correct ratio between λ_0 and total bunch length. There are additional complications arising from the longitudinal slice energy spread and initial bunch's chirp (both features are influenced by the RF-gun laser-launch phase, field on cathode surface and laser spot size and duration). The scheme can be augmented by an additional flexibility, e.g., by selecting the thickness of the DLW to enable the excitation of multiple modes.

As an illustrative example we consider a DLW with dimensions $(a,b) = (1\text{ mm}, 1.45\text{ mm})$ and with a 20-cm length located 1 m downstream of the photocathode. We note that the use of a shorter DLW is also possible but would reduce the induced energy modulation and would therefore require a longer drift length to generate a similar current distribution). Figure 2 (left) presents snapshots of the longitudinal-phase space and associated current downstream of the DLW. Additionally Fig. 2 (right) shows the calculated maximum accelerating field E_+ and transformer ratio $\mathscr{R} = E_+/E_-$ as a function of the drift length downstream of the DLW. Here $\mathscr{R}$ and E_+ are computed by considering the shape achieved along the drift and convolving them with the Green's function associated to the wake produced in a cylindrical-symmetric DLW with dimensions $(a,b) = (165\ \mu\text{m}, 195\ \mu\text{m})$ and relative permittivity $\varepsilon_r = 5.7$.

ECHO-ENABLED HARMONIC GENERATION

Another interesting possibility to explore is echo enabled harmonic generation (EEHG). In the conventional two-stage EEHG technique, an ultra relativistic electron bunch is energy modulated with a laser in an undulator (the laser-undulator system is henceforth refer to as "energy modulator"). The frequency of the modulation corresponds to

the laser-undulator resonant wavelength $f_0^{(1)}$. The bunch then passes through another chicane to locally over-bunch the beam thereby producing a stratified longitudinal phase space. The bunch subsequently interacts with a laser in a second energy modulator yielding the superimposition of an energy modulation with frequency $f_0^{(2)}$. In the last stage of the process the bunch passes through a chicane with R_{56} selected to form very short microbunches. The frequency spectrum of the bunch is peaked at frequencies given by $f_{echo}^{m,n} = mf_0^{(1)} + nf_0^{(2)}$ with $n, m \in \mathbb{N}$.

Here we note that a DLW structure with a proper fundamental mode can replace the laser and undulator system in EEHG configuration albeit at the price of longer modulation wavelength. We continue considering the setup described in this paper and take the case of a non ultra-relativistic bunch. In such a case, a drift space with proper length between the modulators plays the same roles as the chicane in the conventional EEHG. We note that the idea of using an EEHG scheme to micro bunch non-relativistic beams was recently proposed in high-power W-band sources [20].

Considering the same configuration studied in the previous section, the ~ 5 MeV bunch produced by the RF gun is injected in two successive DLW structures. We choose the fundamental frequencies of the first and second DLWs to be respectively $f_0^{(1)} = 0.6$ and $f_0^{(2)} = 0.4$ THz. This choice corresponds to the parameters $(a, b, \varepsilon, L) =$ (0.4 mm, 0.43 mm, 5.7, 10 cm) and $(a, b, \varepsilon, L) =$ (0.5 mm, 0.55 mm, 5.7, 5 cm) for the first and second DLW structures respectively. The resulting longitudinal phase spaces and current densities are shown in Fig. 3 and demonstrate the capability of the system to support a EEHG-like harmonic bunching scheme.

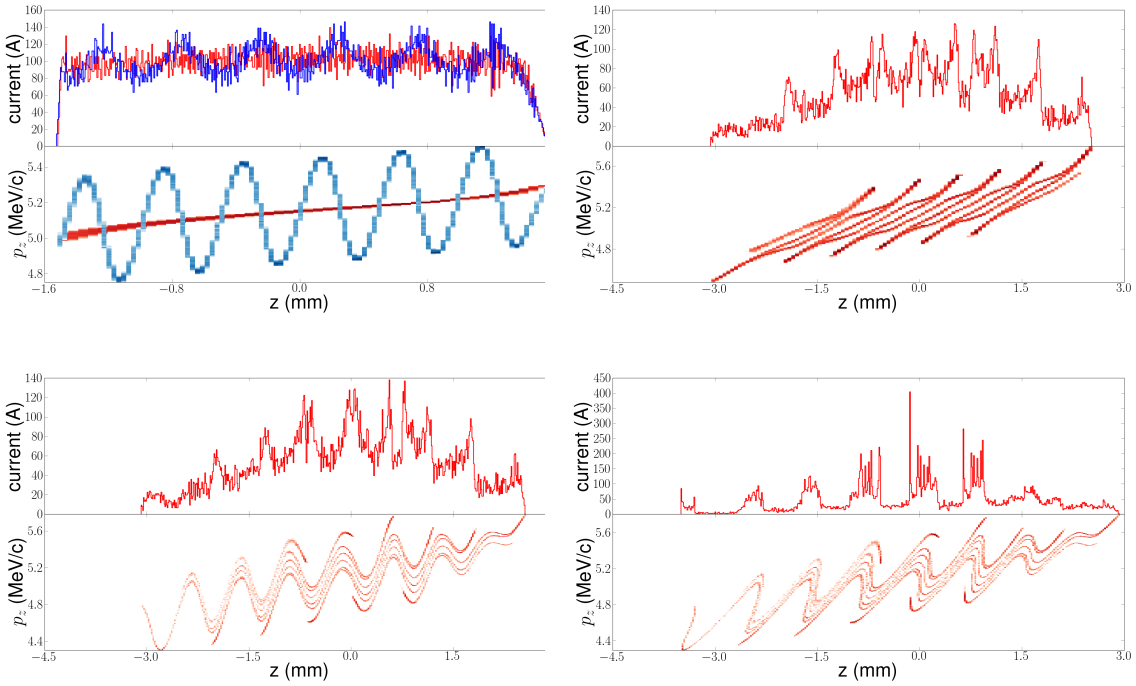

FIGURE 3. Generation of EEHG with two DLWs: A plateau distribution is shown immediately before (red trace) and after (blue trace) passing through a DLW with $f_0^{(1)} = 0.6$ THz (top left). A snapshot of the bunch after a 1.6 m drift (top right) before entering the second DLW with $f_0^{(2)} = 0.4\,THz$. Finally, the bunch is shown immediately after the second DLW (lower left), and after a 25 cm drift (lower right). In each figure the longitudinal phase space and current distributions are shown (as lower and upper sub-plots respectively).

The quality of the bunching can be further quantified by introducing the bunch form factor (BFF) defined as $\widetilde{F}(\omega) = N^{-2}\left|\sum_{k=1}^{N} e^{-i\omega z_k/c}\right|^2$ where the summation is carried over the number of macro particles N. The evolution of $\widetilde{F}(\omega)$ as a function of the distance from the exit of the second DLW is shown in Fig. 4 for the same case as the one presented in Fig. 3. The BFF is enhanced at $f_0^{(2)}$ and its second harmonic at 0.8 THz. In addition we observe peaks at

"echo" harmonics appearing as "islands" located at 1, 1.4, and 1.8 THz in Fig. 4. These frequencies are given from the "echo" unconverted frequency $f_{echo}^{m,n} = mf_0^{(1)} + nf_0^{(2)}$ with $m = 1$ and $n = 1, 2, 3$ respectively.

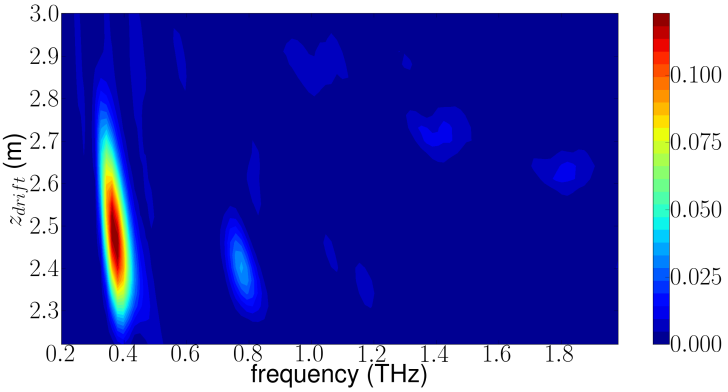

FIGURE 4. BFF evolution downstream of the second DLW for the same configuration as presented in Fig. 3.

ACKNOWLEDGMENTS

This work was supported by the Defense Threat Reduction Agency, Basic Research Award # HDTRA1-10-1-0051, to Northern Illinois University, by US DOE contracts No. DE-SC0011831 to Northern Illinois University and DE-AC02-07CH11359 to the Fermi research alliance LLC.

REFERENCES

1. B. O'Shea, These proceedings.
2. F. Lemery, P. Piot, "Ballistic Bunching of Photo-Injected Electron Bunches with Dielectric-Lined Waveguides", preprint arXiv:1407.1005 [physics.acc-ph] (2014).
3. S. Antipov, C. Jing, P. Schoessow, A. Kanareykin, B. Jiang, V. Yakimenko, A. Zholents, and W. Gai, AIP Conf. Proc. **1507**, 421 (2012).
4. S. Antipov, M. Babzien, C. Jing, M. Fedurin, W. Gai, A. Kanareykin, K. Kusche, V. Yakimenko, and A. Zholents, Phys. Rev. Lett. **111**, 134802 (2013)
5. S. Antipov, C. Jing, P. Schoessow, A. Kanareykin, B. Jiang, V. Yakimenko, A. Zholents, and W. Gai, Rev. Sci. Instrum. **84**, 022706 (2013)
6. G. Stupakov, Phys. Rev. Lett. **102**, 074801 (2009).
7. D. T. Palmer, R. H. Miller, H. Winick, X.J. Wang, K. Batchelor, M. Woodle, and I. Ben-Zvi, "Microwave measurements of the BNL/SLAC/UCLA 1.6-cell photocathode RF gun", in Proceedings of the 1995 Particle Accelerator Conference, PAC'95 (Dallas, TX, 1995), 982 (1996).
8. M. Rosing, and W. Gai, Phys. Rev. D **42**, 1829 (1990).
9. K. Flöttmann, ASTRA*: A space charge algorithm, User's Manual*, available from the world wide web at http://www.desy.de/∼mpyflo/AstraDokumentation (unpublished).
10. X. J. Wang, , X. Qiu, and I. Ben-Zvi, Phys. Rev. E **54** R3121 (1996).
11. X. J. Wang, X. Y. Chang, Nucl. Instr. Meth. A **507** 310 (2003).
12. P. Piot, L. Carr, W. S. Graves, and H. Loos, Phys. Rev. ST Accel. Beams **6**, 033503 (2003).
13. M. Ferrario, et al. Phys. Rev. Lett. **104** 054801 (2010).
14. T. van Oudheusden, P. L. E. M. Pasmans, S. B. van der Geer, M. J. de Loos, M. J. van der Wiel, and O. J. Luiten, Phys. Rev. Lett. **105**, 264801 (2010)
15. P. Muggli, V. Yakimenko, M. Babzien, E. Kallos, and K. P. Kusche, Phy. Rev. Lett. **101**, 054801 (2008).
16. S. Antipov, These proceedings.
17. P. Piot, Y.-E Sun, T. J. Maxwell, J. Ruan, A. H. Lumpkin, M. M. Rihaoui, and R. Thurman-Keup, Appl. Phys. Lett. **98**, 261501 (2011).
18. R. J. England, J. B. Rosenzweig, and G. Travish, *Phys. Rev. Lett.* **100**, 214802 (2008).
19. P. Piot, C. Behrens, C. Gerth, M. Dohlus, F. Lemery, D. Mihalcea, P. Stoltz, M. Vogt, Phys. Rev. Lett. **108**, 034801 (2012).
20. H Gong, G. Travish, J. Xu, Y. Wei, J. Feng and Y. Gong, Phys. Plasmas **20**, 013303 (2013).